ELSEVIER

Thermochimica Acta 391 (2002) 279–295

thermochimica acta

www.elsevier.com/locate/tca

About the changes of heat capacity, glass transition temperature and relaxation time during the polymerization reaction of thermosetting systems

Jürgen E.K. Schawe*

Mettler-Toledo GmbH, Sonnenbergstrasse 74, CH-8603 Schwerzenbach, Switzerland

Received 12 July 2001; accepted 9 November 2001

Abstract

During molecular growth reactions, molecular mobility decreases. Experimentally, an increase in the relaxation time can be detected in the course of isothermal network formation. This process was studied by differential scanning calorimetry (DSC) and temperature modulated DSC using the curing reaction of an epoxy-amine thermosetting system as a classic example. In particular, the conversion dependence of the relaxation time, the heat capacity and the glass transition temperature were investigated. Molecular details of the reaction, i.e. the relaxation and the vitrification are discussed. It is shown, that the change in relaxation behavior during the isothermal cross-linking of chemically unstable material can be described in the same way as the virtual cooling experiment of chemically stable material. Based on this concept, a new relationship for the conversion dependence of the glass transition temperature is derived. It appears that the change of the glass transition temperature as a function of the conversion is directly related to the molecular relaxation processes.

Keywords: Curing reaction; Heat capacity; Glass transition; Relaxation; Vitrification

1. Introduction

The investigation of dynamic processes during chemical reactions is a frequently used application of differential scanning calorimetry (DSC). Two important advantages of the DSC technique are the relatively simple sample preparation and the short measurement time. In contrast, the interpretation of the measurement curves is sometimes difficult. Besides this, the quantitative determination of thermodynamic properties is not so easy in some cases because of the complex influence of the heat transfer on the heat flow curves. The investigation of related methodical problems is one of the important topic described in the work of Höhne. The importance of the evaluation of thermal properties by DSC measurements and the problems involved are discussed in Hemminger and Höhne's first book [1]. Höhne and co-workers [2–6] have also developed other methods for the measurements and for data analysis such as calibration and desmearing. In the case of polymerization (or curing) reactions, it has been shown by Richardson [7,8] that knowledge of the heat capacity during the reaction is important in order to evaluate the DSC curves properly.

The introduction of temperature modulated DSC (TMDSC) [9–12] allowed the heat capacity and of the heat of reaction to be simultaneously measured. This possibility was first employed by Cassettari et al. [11] to study the thermal relaxation behavior during

* Fax: +41-1806-7240.
E-mail address: juergen.schawe@mt.com (J.E.K. Schawe).

0040-6031/02/$ – see front matter
PII: S0040-6031(02)00190-9

Nomenclature

A_0	constant
B	curvature parameter in the Vogel–Fulcher equation
c_p	specific heat capacity at constant pressure
c_{p1}	c_p in the liquid state
c_v	specific heat capacity at constant volume
c^*	complex specific heat capacity
c'	real part of the complex specific heat capacity
c''	imaginary part of the complex specific heat capacity
Δc_{p0}	step in the specific heat capacity at the glass transition of uncured material
Δc_{p1}	step in the specific heat capacity at the glass transition of fully cured material
Δc_ξ	difference of the specific heat capacity of the liquid state between a fully cured and an uncured material
C_2	temperature difference between T_g and T_v (WLF parameter)
D	fragility parameter
f	frequency
Δh	specific enthalpy
Δh_r	specific reaction enthalpy
$\Delta(\log \tau_0)$	difference of the logarithm from τ_0 and τ_{s0}
m	sample mass
R	universal gas constant
t	time
t_{end}	maximum time of an isothermal (or quasi-isothermal) measurement
t_p	period
t_{react}	reaction time
t_v	vitrification time
t_τ	characteristic time of the relaxation during an isothermal chemical reaction measured at the frequency, $f = 1/2\pi\tau$
T	temperature
T_g	glass transition temperature (measured with a DSC at 10 K/min)
T_{g1}	glass transition temperature of the fully cured material
T_{g0}	glass transition temperature of uncured material
T_m	melting temperature
T_v	Vogel temperature
$T_{\tau 0}$	temperature of the relaxation transition of uncured material measured at the frequency, $f = 1/2\pi\tau = 24$ mHz
$T_{\tau 1}$	temperature of the relaxation transition of fully cured material measured at the frequency, $f = 1/2\pi\tau = 24$ mHz
T_ϕ	actual temperature of the fictive cooling process, which describes the change of τ during an isothermal reaction
x_0	parameter

Greek letters

λ	parameter of the DiBenedetto equation
ξ	conversion
ξ_p	conversion measured in a post-curing experiment after an isothermal (or quasi-isothermal) measurement
τ	relaxation time
τ_s	conversion dependent relaxation time in an isothermal curing reaction which is shifted to the activation curve of the uncured material (relaxation time during a fictive cooling process)
τ_{s0}	relaxation time at the initial conditions (curing temperature and $\xi = 0$) of the fictive cooling process
τ_0	pre-exponential factor in the Vogel–Fulcher equation
Φ_u	underlying heat flow
$\omega = 2\pi f$	angular frequency

reactions. In a different approach, Van Assche et al. [13,14] used TMDSC to analyze the change of the reaction kinetics from a chemically controlled to a diffusion controlled reaction. In the present paper, the behavior of the heat capacity and the glass transition temperature during polymerization are discussed.

From conventional DSC measurements it is well known that the glass transition temperature depends on the conversion of the curing reaction of thermosetting systems [15]. As shown by Ferrari et al. [16] and later by Schawe and Alig [17], the heat capacity change during the isothermal network formation of a

thermosetting system can be interpreted as a relaxation process. In Ref. [17] the heat capacity relaxation is described as a chemically induced relaxation process in an equilibrated liquid. An extension of this concept to a non-equilibrated vitrification process is given in [18]. Here the thermal relaxation and vitrification process during isothermal curing reaction is described as a fictive cooling experiment of a chemically stable material.

Based on measurements of the thermal relaxation, the following aspects of the curing reaction of a thermosetting system and vitrification are discussed in this article:

(i) the behavior of the heat capacity as a function of conversion before the relaxation transition occurs;
(ii) the reaction time dependence of the relaxation (TTT diagram);
(iii) the conversion dependence of the relaxation time and the glass transition temperature.

It is shown that the increase of the glass transition temperature during a curing reaction can be understood as being a consequence of changes in the relaxation behavior. The actual thermal relaxation behavior can be modeled by applying a simple scaling concept. As a result, we present a novel description for the reaction dependence of the glass transition temperature.

2. Experimental

2.1. Samples

Samples were prepared using DGEBA (Epikote 828, supplied by Shell Chemical)with $n = 0.14$ and

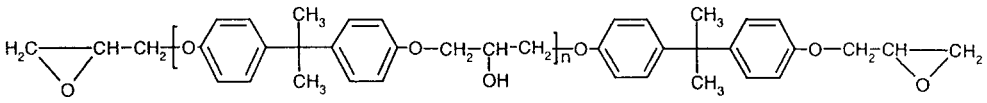

DDM (supplied by Aldrich).

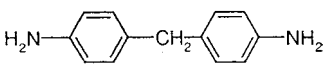

The substances were mixed in stoichiometric amounts (2 mol DGEBA and 1 mol DDM) at 120 °C, stirred for 20 s and then cooled rapidly at room temperature. The molar masses of DGEBA and DDM are 379.7 and 198 g/mol respectively. The molar mass of the mixture is therefore 319.1 g/mol. Samples of 2–5 mg were filled in aluminum crucibles and stored below −35 °C before measurement. Regular measurements of the reaction enthalpy with DSC were carried out to check the stability of the samples. No reaction was detected in the period during which the investigations were performed.

2.2. Instrumental

DSC and TMDSC measurements were performed using a Mettler-Toledo DSC 821e module with the STAR^e software. The instrument was calibrated with water, indium and tin standards.

In TMDSC measurements, the temperature program is given by overlaying a conventional temperature program (linear heating or cooling or isothermal conditions) with a small sinusoidal temperature perturbation characterized by an amplitude and period t_p or frequency, $f = 1/t_p$. This technique is described in detail in Refs. [12,19–21] and the references within. For the TMDSC technique, the underlying (or total heat flow) and the real part of the complex heat capacity are evaluated. The calibration of the complex heat capacity for quasi-isothermal measurements by TMDSC is described in [22].

TMDSC measurements were performed under quasi-isothermal conditions or using a heating rate of 0.5 K/min. The temperature amplitude was 0.5 K except for measurements with periods of less than 24 s, in which case the temperature amplitude was 0.1 K.

3. Results and discussion

3.1. Thermal relaxation of chemically stable material

One way to measure thermal relaxation behavior is with a TMDSC experiment using a small underlying

heating rate. From the periodic component of the heat flow rate the complex heat capacity c^* can be determined [13,20]

$$c^*(\omega) = c'(\omega) - \mathrm{i}c''(\omega) \quad (1)$$

Here c' is the real part and c'' denotes the imaginary part of c^*; the imaginary unit is i. In general, the complex heat capacity depends on the frequency, $f = \omega/2\pi = 1/t_p$ (ω is the angular frequency and t_p the period).

During a thermal relaxation transition the real part c' changes stepwise and the imaginary part c'' shows a peak. The temperature at the inflection point of the c' step or the peak maximum in c'' is characteristic for the relaxation process. To a good approximation, at these points $\omega\tau = 1$, where τ is a characteristic relaxation time. At higher frequencies the inflection point of the c'-curve shifts to higher temperatures. The related curves for the non-cross-linked DGEBA sample are shown in Fig. 1. In analogy to mechanical and dielectric investigations, the temperature dependence of the relaxation time above the vitrification range can be described by the Vogel–Fulcher (VF) equation [23,24]:

$$\log\tau = \log\tau_0 + \left(\frac{B}{T - T_\mathrm{v}}\right) \quad (2)$$

where τ_0 is the pre-exponential factor, B the curvature parameter and T_v the Vogel temperature. B can be expressed by the fragility parameter D [25]:

$$\log\tau = \log\tau_0 + \left(\frac{DT_\mathrm{v}}{T - T_\mathrm{v}}\right) \quad (3)$$

For the Vogel temperature we assume that

$$T_\mathrm{v} = T_\mathrm{g} - C_2 \quad (4)$$

where T_g is the glass transition temperature (measured by conventional DSC at 10 K/min) and C_2 is a parameter in the order of 50 K. In contrast to a simple thermally activated process (Arrhenius behavior), Eq. (3) describes a non-linear curve in the activation diagram ($\log\tau$ versus reciprocal temperature). Such behavior is typical for cooperative relaxation processes.

To determine the VF parameters, TMDSC and dielectric data (from [17,18]) are plotted together in an activation diagram. The fit of these data with the VF equation is shown in Fig. 2. The parameters are $\log\tau_0 = -14.3$, $D = 2.175$, $B = 490.3$ K and $C_2 = 29.4$ K. The glass transition temperature T_g measured by conventional DSC was found to be 258.1 K. It is known that the curves in the activation diagram measured by different techniques are not identical [26,27]. It should also be noted that the data obtained from dielectric analysis might give slightly lower relaxation times (up to 1 decade) compared with the relaxation times measured by calorimetric methods [28,29]. This is the reason for the experimental uncertainty in the determination of the VF parameter when dielectric

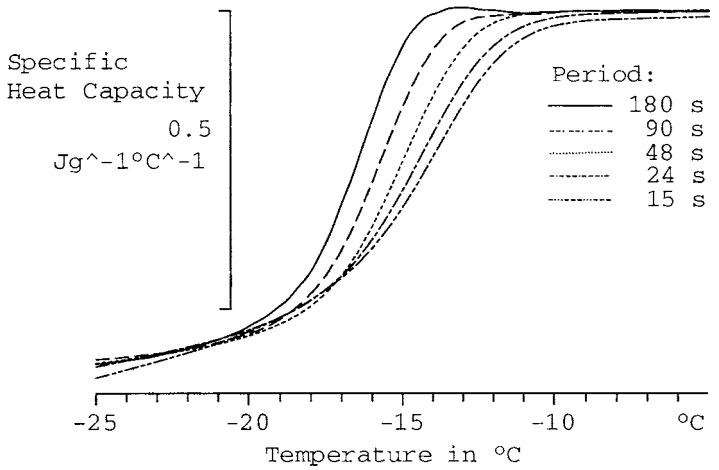

Fig. 1. Real part of the specific complex heat capacity in the glass transition range of the uncured material measured at different periods. Underlying heating rate: 0.5 K/min; temperature amplitude: 0.5 K; sample mass: 9.82 mg.

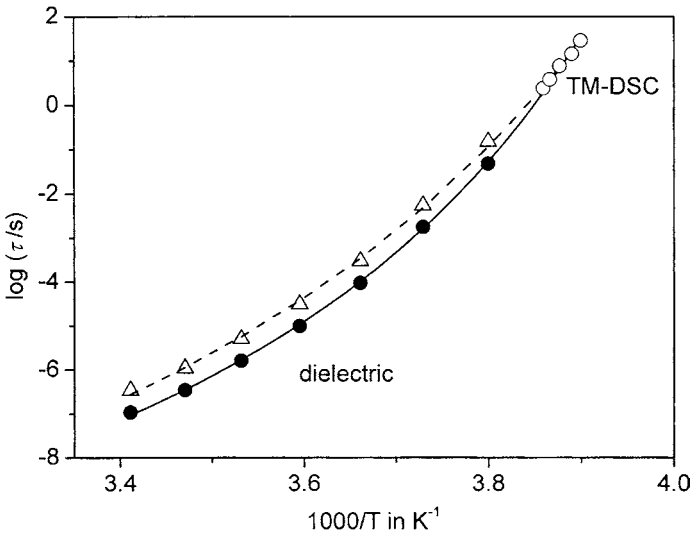

Fig. 2. Logarithm of the relaxation time as a function of the reciprocal temperature (activation diagram) for uncured material. The filled circles are results from dielectric measurements. The open circles are from TMDSC measurements. The lines represent fit curves using the VF equation. The triangles and dashed curve are from shifted dielectric data (for explanation see the text).

and thermal relaxation times are simultaneously used for curve fitting. To illustrate the related uncertainty of the VF parameters, we shift the dielectric data of τ half a decade to higher values (unfilled symbols in Fig. 2). The result of the fit with the VF equation are: $\log \tau_0 = -15.4$, $D = 3.135$, $B = 677.8$ K and $C_2 = 41.9$ K.

3.2. Conventional DSC measurements of the glass transition and the conversion

With conventional DSC it is possible to determine the glass transition temperature and the degree of conversion related to a previous isothermal reaction in a set of dynamic scan experiments [30]. Samples of the fresh (initial) mixture (DGEBA–DDM) were cured isothermally at 100 °C for different periods of time. The samples were then cooled rapidly to −30 °C and then measured at a heating rate of 10 K/min. The results are shown in Fig. 3. For reference purposes, the curves of pure DGEBA and of the fully cured material (second run) are also shown in the same figure.

The curves first show a step in the heat flow due to the glass transition. The curing reaction then begins and gives rise to the exothermic peak. With curing times longer than 40 min the glass transition is accompanied by an enthalpy relaxation peak.

Increasing the reaction time shifts the glass transition to higher temperatures and the area of the reaction peak decreases. From the peak area the conversion ξ at the different reaction times t_{react} can be calculated:

$$\xi(t_{\text{react}}) = \frac{\Delta h(t_{\text{react}})}{\Delta h_{\text{r}}} \tag{5}$$

where Δh is the specific enthalpy determined from the actual area of the reaction peak and Δh_{r} is the specific enthalpy of reaction (determined from the heating run of the initial mixture at 10 K/min). Δh_{r} was determined to be 406 J/g.

The change of the glass transition temperature and the conversion during the course of the reaction determined from the curves in Fig. 3 are plotted in Fig. 4. The resulting function $T_{\text{g}}(\xi)$ is also included in this figure.

During the curing reaction, the initial low molecular weight mixture is transformed into a polymer network. With increasing molecular weight, the glass transition temperature (vitrification temperature) increases. If the actual vitrification temperature is in the range of the curing temperature, the material vitrifies during the reaction. As a result of this, the reaction becomes diffusion controlled. The time at which the glass transition temperature equals the reaction temperature is defined as vitrification time, t_{v} (Fig. 4). After the

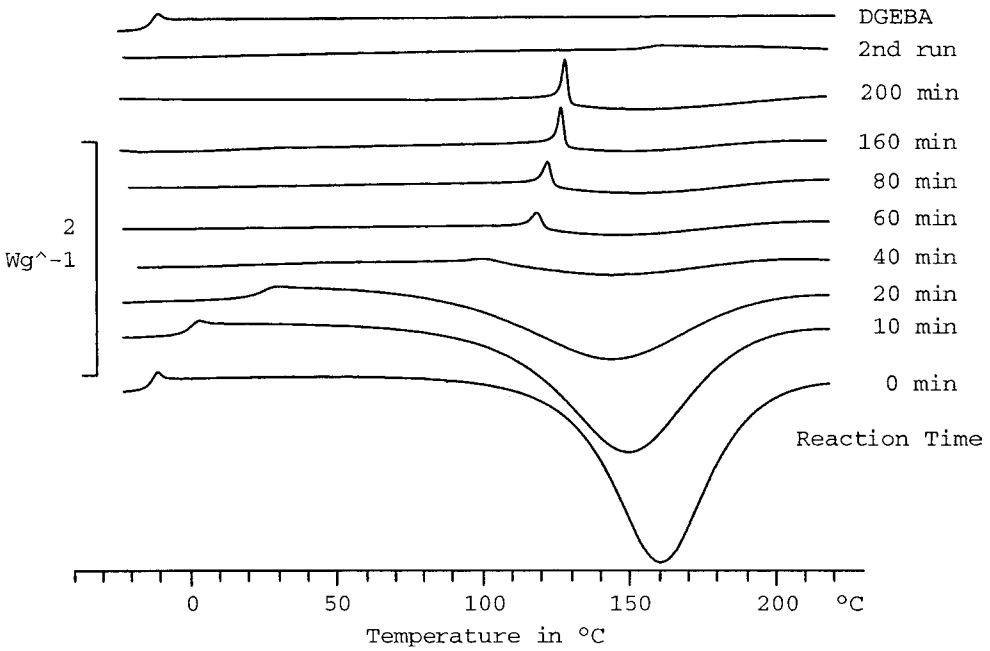

Fig. 3. Conventional DSC curves measured at 10 K/min after longer periods of isothermal curing at 100 °C followed by rapid cooling to −30 °C. The curves of the pure DGEBA and the fully cured material (second run) are plotted in the diagram.

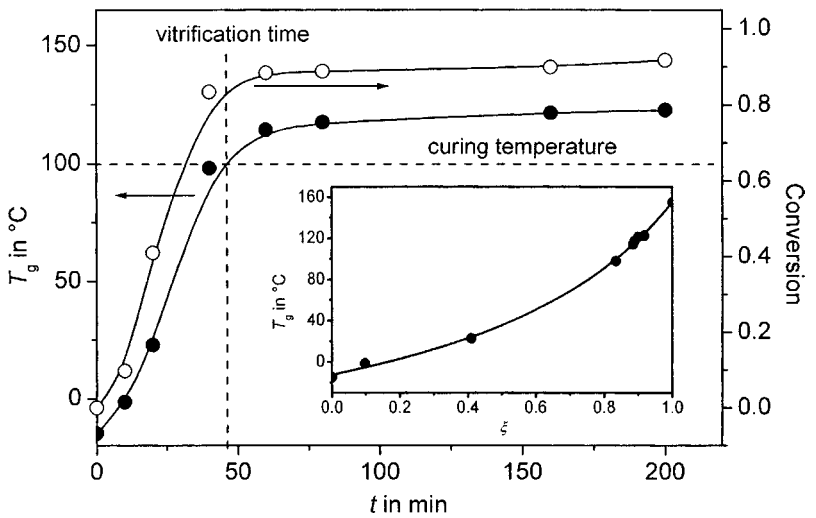

Fig. 4. The glass transition temperature and conversion as a function of the reaction time during curing at 100 °C. The data are determined from the curves in Fig. 3. The inset diagram shows a plot of the resulting dependence of the glass transition temperature on the conversion.

vitrification time, the reaction rate (and the change in the glass transition) slow down.

3.3. Thermal relaxation and the temperature–time-transition (TTT) diagram

To study the thermal relaxation during the reaction, quasi-isothermal TMDSC measurements were performed in the temperature range 40–170 °C. The measurements were repeated with a fresh sample at intervals of 10 K. A frequency of 42 mHz ($t_p = 24$ s) was used. The sample was put in the preheated sample holder immediately before each measurement. After the quasi-isothermal measurement, the sample was cooled down rapidly to room temperature and a conventional DSC heating run performed at 10 K/min to measure the post-curing behavior.

The underlying heat flow (total heat flow) and the real part of the complex heat capacity were determined from the measurement curves. A number of such curves are shown in Fig. 5. After a small increase, the heat capacity decreases in a step-like fashion during the reaction. This can be interpreted as being a result of the vitrification process due to molecular growth. As described in Refs. [17,22,31], we attribute this process to chemically induced thermal relaxation. This explains the phenomenon that the step in the heat capacity signal is frequency dependent. This is shown in Fig. 6 for the c'-curves measured during a quasi-isothermal reaction at 120 °C at different frequencies.

Below 140 °C an increase in the reaction temperature causes thermal relaxation process to shift to shorter reaction times. Above 140 °C the step-height of c' decreases significantly because at these temperatures the fast components of the cooperative process are so fast that they do not contribute to the chemically induced relaxation process at the respective frequency. As the temperature increases the contribution of the cooperative process decreases. Above 170 °C the cooperative motions are so fast that no relaxation is possible at the applied frequency.

In the literature [32,33] these kinds of heat capacity curves are used to construct TTT diagrams [34]. In such diagrams the reaction temperature is plotted as a function of the vitrification time. The transition from the liquid to the glassy state during reaction is thus

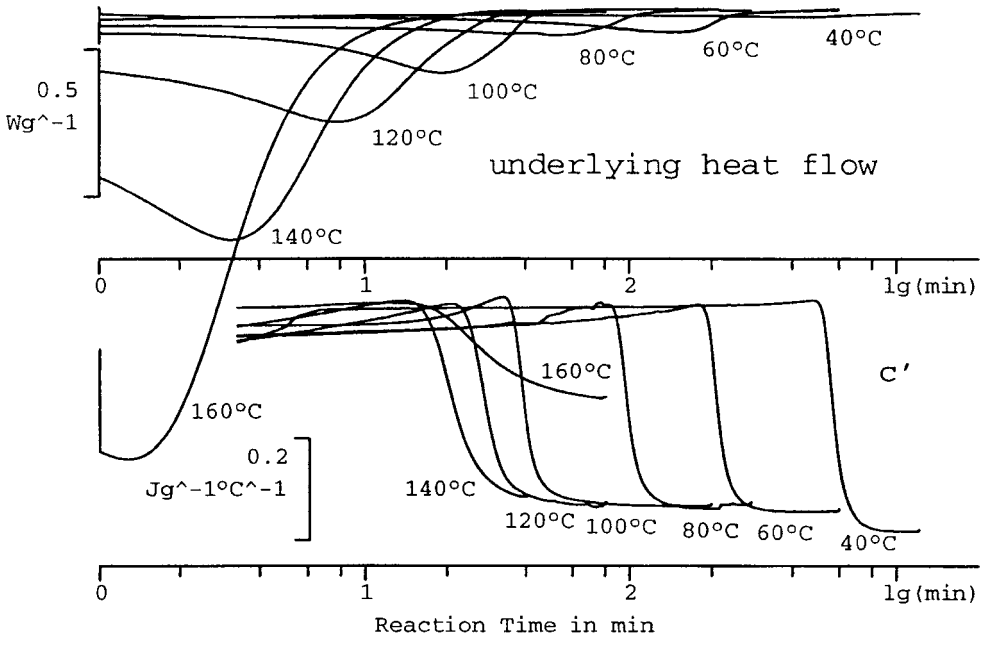

Fig. 5. Selected curves of the underlying heat flow and real part of the specific complex heat capacity c' measured by TMDSC during quasi-isothermal curing at a temperature amplitude of 0.5 K and a period of 24 s (frequency: 42 mHz). The measurements were performed between 40 and 170 °C. The parameter is the reaction temperature. The sample mass was approximately 3 mg.

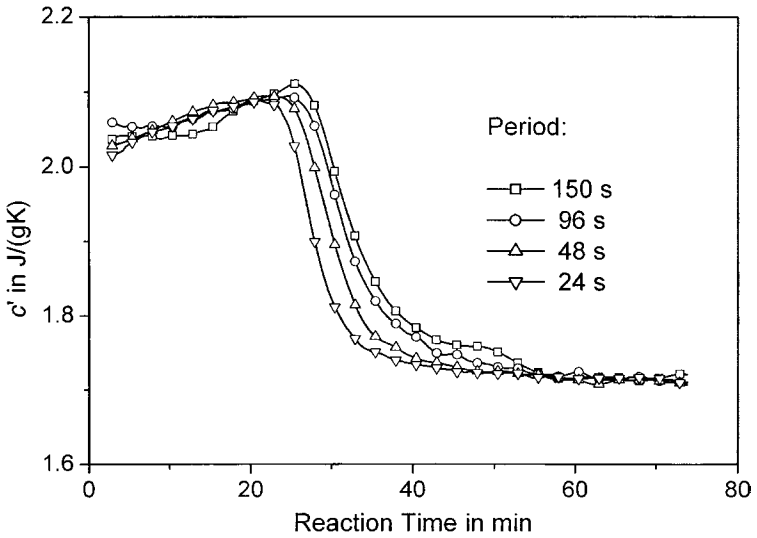

Fig. 6. The real part of the specific complex heat capacity measured during quasi-isothermal curing at 120 °C by TMDSC at different periods. The temperature amplitude was 0.5 K and the typical sample mass was 3 mg.

described. The vitrification time characterizes the transition of the sample from the liquid to the glassy state. This process depends on the degree of conversion and the temperature. The static heat capacity drops down to the value of that of the solid material and the reaction becomes diffusion controlled. This process is independent of the measurement frequency. In contrast, the heat capacity step measured by TMDSC is frequency dependent. On increasing the frequency, the measured step shifts to lower times [31]. The characteristic time for the step in c' is therefore not identical to the vitrification time t_v. We therefore replace t_v by the time of the relaxation transition at a given frequency t_τ. This time is commonly used to construct the TTT diagram on the basis of TMDSC data [32,33]. However, t_τ is not identical to the vitrification time t_v. In this paper t_τ is defined as the reaction time at which the heat capacity step has the half step-height. Using this data we obtain the TTT diagram as shown in Fig. 7. Since the frequency is 42 mHz, the related relaxation time, $\tau = 1/2\pi f$ is 3.8 s.

In principle, the time of the relaxation transition t_τ is less than the vitrification time t_v. However, the determination of t_v by post-curing experiments with conventional DSC as described below is time consuming and the accuracy of the t_v values is relatively low. It is therefore advantageous to use TMDSC measurements to construct TTT diagrams. To show the differences between the t_τ and t_v values, the vitrification times determined from post-curing experiments at 80 and 100 °C are also plotted in Fig. 7. At these temperatures the deviations of t_τ and t_v can be neglected for most practical purposes.

3.4. The conversion dependence of the heat capacity during isothermal reaction

Before the relaxation transition the heat capacity increases slightly (Fig. 5). This behavior corresponds to the initial period of curing and is interpreted as an increase of configurational and/or vibrational contributions in the liquid state due to network growth [16]. Here we will investigate this effect in more detail by analyzing the conversion dependence of the heat capacity. To do this we first have to determine the time dependence of the conversion, ξ. The main problem involved in the determination of ξ is that for isothermal measurements the reaction may already proceed before the measurement actually begins. To reduce such uncertainties we perform a conventional DSC experiment directly after the quasi-isothermal TMDSC measurement. The remaining unreacted part ξ_p is determined form the post-curing curve using

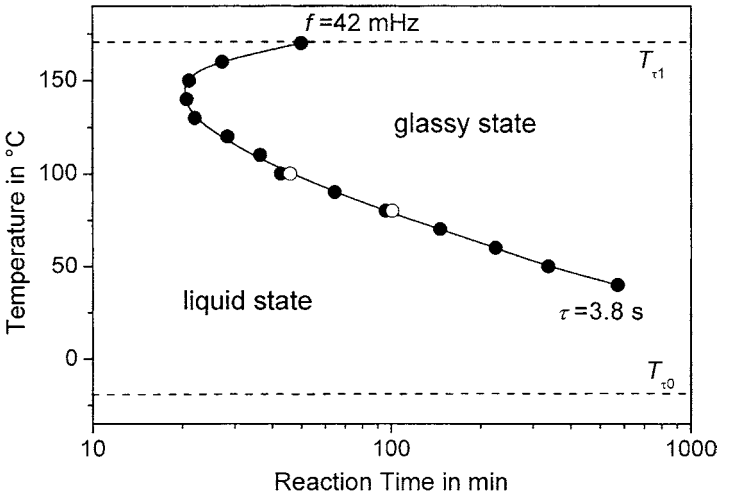

Fig. 7. TTT diagram for the isothermal curing of the DGEBA–DDM system using the data from quasi-isothermal TMDSC measurements (Fig. 5). For comparison, the data taken from conventional DSC measurements (Figs. 3 and 4) for curing temperatures of 80 and 100 °C are plotted in this diagram (open circles).

Eq. (5). The conversion can then be calculated as a function of the reaction time by the equation

$$\xi(t_{\mathrm{react}}) = 1 - \xi_{\mathrm{p}} + \frac{1}{m\Delta h_{\mathrm{r}}} \times \left(\int_0^{t_{\mathrm{react}}} \Phi_{\mathrm{u}}(t')\,\mathrm{d}t' - \int_0^{t_{\mathrm{end}}} \Phi_{\mathrm{u}}(t')\,\mathrm{d}t' \right) \quad (6)$$

where Φ_{u} is the underlying heat flow measured in the quasi-isothermal TMDSC experiment and t_{end} is the reaction time of the isothermal reaction. The conversion versus the reaction time is shown in Fig. 8. Using this data the heat capacity can be plotted as a function of the conversion, as shown in Fig. 9. Before the relaxation transition, the heat capacity increases linearly with

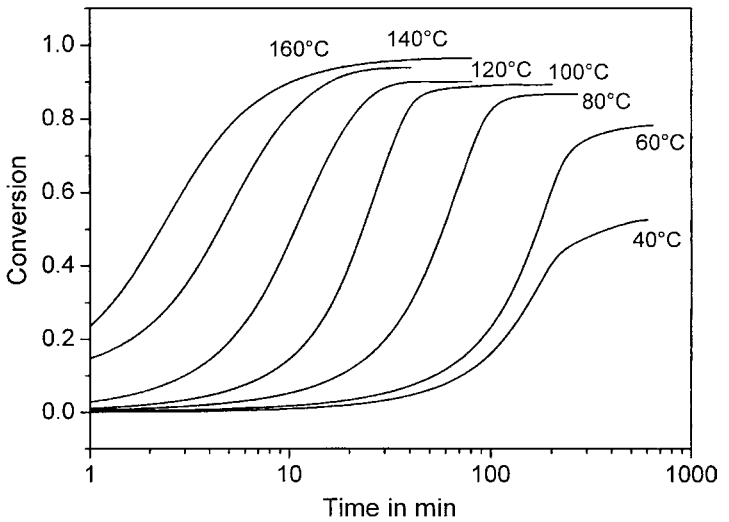

Fig. 8. Conversion versus reaction time as a result of the quasi-isothermal TMDSC measurements (Fig. 5). The parameter is the reaction temperature.

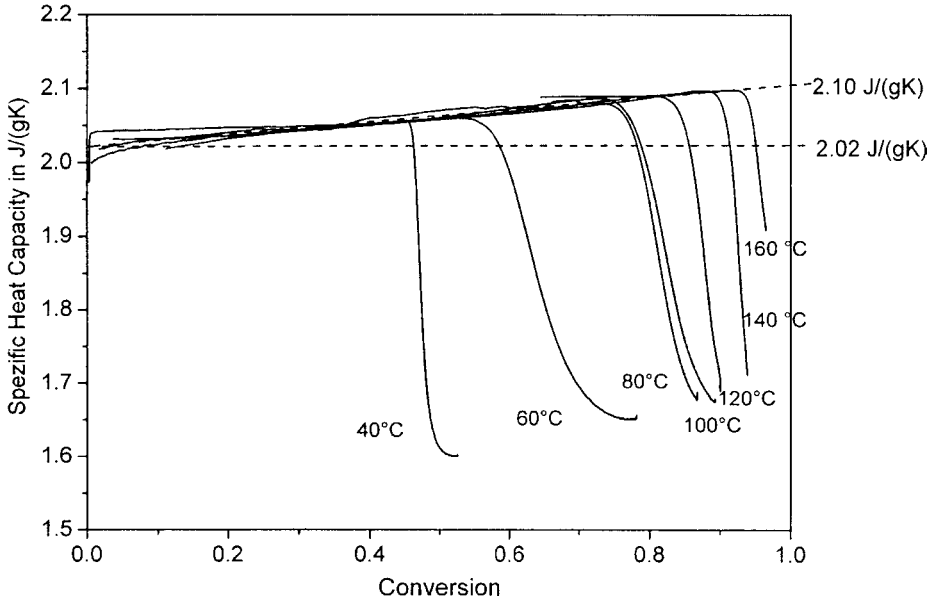

Fig. 9. The specific heat capacity as a function of conversion different reaction temperatures. The curves are evaluated from the curves in Fig. 5. The parameter is the reaction temperature.

conversion. In this range, a linear change in the heat capacity of the liquid sample during reaction is indicated. This linear dependence is characterized by a dashed line in Fig. 9. From this line we can estimate the specific heat capacity of the uncured ($\xi = 0$) liquid to be 2.02 J/g K. For the specific heat capacity of the fully reacted sample ($\xi = 1$) we determine $c'(\xi = 1) =$ 2.10 J/g K by linear extrapolation. The heat capacity of the liquid as a function of conversion can thus be approximated by

$$c_{p1}(\xi) = c_{p1}(\xi = 0) + \left(\frac{\partial c_{p1}}{\partial \xi}\right)_T \xi \tag{7}$$

The maximum change in the heat capacity of the liquid due to reaction is

$$\Delta c_{p1}\left(\frac{\partial c_{p1}}{\partial \xi}\right)_T = 0.08\,\mathrm{J/g\,K}$$

Since 1 mol of the initial mixture contains 2/3 mol DGEBA and 1/3 mol DDM, the molar mass of the initial mixture is 319.2 g. Consequently, the heat capacity difference of the liquid state between an uncured and a fully cured sample is $\Delta c_\xi = 25.5$ J/mol K.

At a sufficiently high temperature for a three dimensional lattice we expect a specific heat capacity at constant volume of $c_v = 3R = 24.9$ J/mol K (R is the gas constant) ([35] and references within). Wunderlich and co-workers [35,36] recommend for the estimation of the heat capacity at constant pressure c_p from c_v for polymers the approximation

$$c_p = c_v + 3RA_0c_p\frac{T}{T_\mathrm{m}} \tag{8}$$

where $A_0 = 3.9 \times 10^{-3}$ mol K/J is a constant and T_m the melting temperature. Using the approximation that $T_\mathrm{m}/T_\mathrm{g} \approx 1.3$ [37], we estimate the c_p-contribution of a three dimensional lattice with one lattice point per mole to be 26.9 J/mol K, which is in good agreement with the experimentally determined value of $\Delta c_\xi =$ 25.5 J/mol K. Consequently, the change in the heat capacity of the liquid during the curing reaction can be interpreted as the formation of an apparent lattice. For the full reacted material, the apparent lattice has 1 mole lattice point in 1 mol substance. A lattice point can be understood as the covalent bonds between 1 DDM molecule with 2 DGEBA molecule due to network formation. The cross-linking point therefore has three additional vibrational degrees of freedom. In the liquid state all other degrees of freedom are not influenced to any extent by the cross-linking reaction for the thermosetting system under investigation.

4. The conversion dependence of the relaxation time

From $\omega\tau = 1$ the relaxation time of $\tau = 3.8$ s is estimated for the measurements as shown in Fig. 5. From this measurement the temperature and the time for the chemically induced relaxation transition at τ are obtained. The temperature of the relaxation transition is the average temperature of the quasi-isothermal experiment. These data are also used for the construction of the TTT diagram (Fig. 7). From the heat flow curves measured by the quasi-isothermal experiments (Fig. 5), the conversion as a function of time was determined. These curves are plotted in Fig. 8. The conversion at which the chemically induced relaxation occurs is by definition ξ at the time of the relaxation transition t_τ. This value of $\xi(T, t_\tau)$ can be evaluated from Fig. 8, where T is the curve parameter and t_τ the related time. The result of this evaluation is a set of the parameters (T_τ, τ, ξ), where T_τ is the temperature at the relaxation transition characterized by the relaxation time τ. (For the quasi-isothermal investigation, T_τ is identical to the average reaction temperature.) From this set of variables one can generate a set of VF curves using the parameter B, $\log \tau_0$ and C_2 from the uncured material. Because the glass transition temperature T_g is not measured, we have to replace T_g by T_τ in the VF equation. From Eqs. (3) and (4) it follows then for a curve at a given conversion ξ

$$\log \tau(\xi) = \log \tau_0 + \frac{DT_\tau(\xi)}{T(1 + D/\log(\tau_m/\tau_0)) - T_\tau(\xi)} \tag{9}$$

where τ_m (=3.8 s) is the relaxation time given by the measuring frequency ($\omega\tau = 1$).

Mijovic and co-workers [38,39] has shown that for different thermosetting systems the fragility parameter D is almost constant over a large conversion range. We therefore assume that D is conversion independent.

According to previous publications [17,18] the VF parameters $\log \tau_0$ and C_2 can to a good approximation assumed to be constant during the curing reaction. A set of such curves is shown in Fig. 10. The curve set describes the temperature–conversion-behavior of the relaxation time to a good approximation [18] and corresponds to the concept of the temperature and

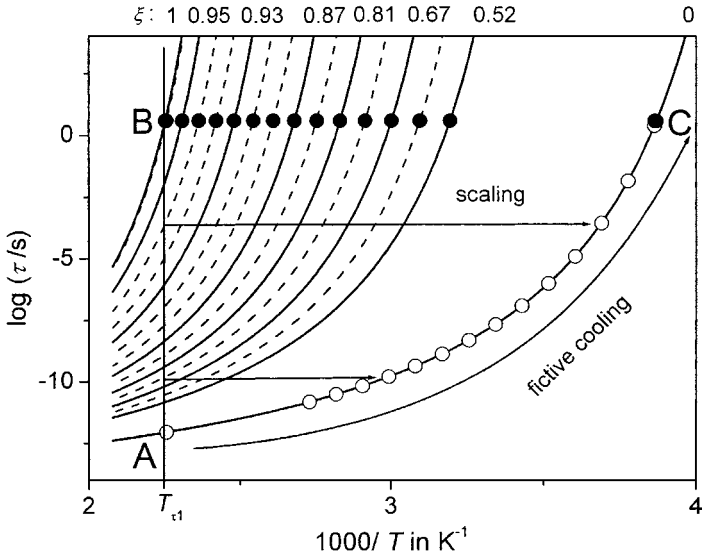

Fig. 10. Curves of the relaxation time at different conversion in the activation diagram. The filled circles are determined from the quasi-isothermal TMDSC measurements (Fig. 5). The curves are calculated with the VF equation using the parameters of the uncured material (Fig. 2). The pathway from A to B characterizes the change of the relaxation time during an isothermal curing experiment at the relaxation temperature of the fully cured material. The open circles represent the relaxation time from the isothermal curing process at the pathway from A to B at different conversions scaled to the curve of the uncured material. The pathway from A to C characterizes a fictive cooling experiment of a chemically stable material, which describes the behavior of the relaxation time during reaction.

time evaluation of the relaxation processes during reaction suggested by Johary [40]. The filled circles in Fig. 10 represent data from the curves shown in Fig. 5. On the basis of these curves, the conversion dependence of the relaxation behavior can be derived. To do this we use the model to describe the function $\tau(\xi)$ that the change of the relaxation time is a result of an isothermal curing reaction at the maximum temperature $T_{\tau 1}$ (the temperature of the relaxation transition of the fully cured material).

To describe the conversion dependence of the relaxation time we discuss the change in τ during an isothermal reaction. Because the complete range of the conversion is considered, the relaxation temperature of the fully cured material $T_{\tau 1}$ is used as a reference temperature. The change of the relaxation time during the isothermal curing reaction at $T_{\tau 1}$ is characterized by the pathway from A to B in Fig. 10. In the unreacted liquid the relaxation time at $T_{\tau 1}$ is short (point A) and decreases by several orders of magnitudes during network formation. Point B characterizes the fully cured material. Along the pathway from A to B all activation curves in between are intersected. In Ref. [18] it is shown that the change of τ in an isothermal curing experiment can be described as a fictive cooling experiment. The change of the relaxation time during such a fictive cooling experiment can be determined by scaling the relaxation time at the actual conversion to the activation curve of the initial mixture ($\xi = 0$). In Fig. 10 this scaling is represented by a horizontal shift of the intersection points between the path A–B and the actual activation curve to the activation curve for $\xi = 0$. The results of this scaling procedure are the open circles in Fig. 10. The fictive cooling starts at the point A and finishes at point C. Point C also represents the temperature which corresponds to the relaxation time $\tau = 1/2\pi f$.

The actual relaxation time during the isothermal reaction at $T_{\tau 1}$ is given by the VF equation:

$$\log \tau(\xi) = \log \tau_0 + \left(\frac{D(T_g(\xi) - C_2)}{T_{\tau 1} - T_g(\xi) + C_2} \right) \tag{10}$$

where $T_g(\xi)$ is the glass transition temperature at ξ. For the relaxation time τ_s, which is scaled to the curve at $\xi = 0$, one obtains:

$$\log \tau_s(\xi) = \log \tau_0 + \left(\frac{D(T_{g0} - C_2)}{T_\phi(\xi) - T_{g0} + C_2} \right) \tag{11}$$

where T_{g0} is the glass transition temperature of the uncured material and T_ϕ the unknown actual conversion dependent temperature of the fictive cooling process. By definition $\tau(\xi)$ in Eq. (10) is identical to $\tau_s(\xi)$ in Eq. (11). Consequently, from this one obtains two equations

$$T_\phi(\xi) = \frac{T_{g0} - C_2}{T_g(\xi) - C_2} T_{\tau 1} \tag{12}$$

The fictive cooling rate is the time derivative of T_ϕ:

$$\frac{dT_\phi(\xi)}{dt} = -\frac{T_{g1}(T_{g0} - C_2)}{(T_g(\xi) - C_2)^2} \frac{dT_g(\xi)}{d\xi} \frac{d\xi}{dt} \tag{13}$$

The relaxation time during the fictive cooling experiment τ_s can be calculated by introducing Eq. (12) into Eq. (11). The result of Eq. (10) shows that τ is replaced by τ_s:

$$\log \tau_s(\xi) = \log \tau_0 + \left(\frac{D(T_g(\xi) - C_2)}{T_{\tau 1} - T_g(\xi) + C_2} \right) \tag{14}$$

The related temperature is given by Eq. (12). Eq. (14) describes the relaxation between the relaxation time τ_s and the glass transition temperature T_g. Because the relaxation is measured at T_τ instead at T_g, the glass transition temperature has to be replaced in a similar way as in Eq. (9):

$$\log \tau_s(\xi) = \log \tau_0 + \frac{DT_\tau(\xi)}{T_{\tau 1}(1 + D/\log(\tau_m/\tau_0)) - T_\tau(\xi)} \tag{15}$$

To describe the dependence between the glass transition temperature and the conversion, a relation between τ_s and ξ has to be found. The data of $\log \tau_s$ calculated by Eq. (15) as a function of conversion is plotted in Fig. 11. The error bars represent the variation of τ_s due to the use of the VF parameters which are determined from a best fit of the shifted dielectric data (open triangles in Fig. 2) together with the TMDSC data. Tombari and Johary [41] suggest for a phenomenological relation between $\log \tau$ and ξ a power law with three parameters. First of all we used this power law for the further discussion. However, it was not possible to find a result that was consistent for the derived relations and the experimental data because of the mathematical structure of the power function. An alternative approach on the basis of the Adam–Gibbs theory [42] is suggested by Corezzi [43].

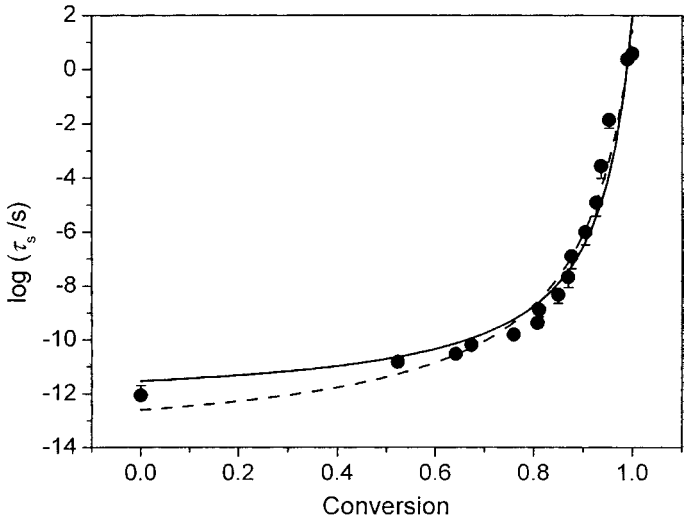

Fig. 11. Conversion dependence of the relaxation time.

Here the conversion dependence of the relaxation time is described by a hyperbolic function. Similarly in this work we prefer to use a relation between $\log \tau_s$ and ξ on the base of a hyperbolic equation:

$$\log \tau_s(\xi) = \log \tau_{s0} + \frac{A}{x_0 - \xi} \tag{16}$$

where τ_{s0} is the relaxation time at the initial conditions and A is a constant. The parameter x_0 characterizes the fictive conversion for the hypothetical case at which the Vogel temperature is equal to the glass transition temperature of the fully cured material. The result of the best fit is $\log \tau_s = -14.1$, $x_0 = 1.105$ and $A = 1.64$. The related curve is the dashed line is shown in Fig. 11. Because the parameter A is close to unity, it is advantageous to reduce the number of parameters in Eq. (16):

$$\log \tau_s(\xi) = \log \tau_{s0} + \frac{1}{x_0 - \xi} \tag{17}$$

The parameters in Eq. (17) are determined by curve fitting (solid line in Fig. 11) to be $\log(\tau_{s0}/s) = -12.5$ and $x_0 = 1.069$. Within the limits of the accuracy of the data, Eq. (17) yields reasonable fit results. We will therefore use this equation from now on.

For simplification, in contrast to Ref. [18] the influence of the non-equilibrium behavior (vitrification) on the relaxation time is neglected. If vitrification occurs, the relaxation time becomes lower and deviates from the VF behavior.

4.1. The relation between the glass transition temperature and conversion

The conversion dependence of the glass transition temperature is discussed in the literature in different ways. Consequently, different relationships are suggested to describe the function $T_g(\xi)$ (e.g. in Ref. [44]). Here we will introduce another equation that is consistent with the model for the relaxation–conversion-behavior as described above.

The starting point for this discussion is given by Eqs. (14) and (17). Combining both equations yields

$$x_0 - \xi = \frac{T_{g1} - T_g(\xi) + C_2}{[\log(\tau_0/\tau_{s0}) \cdot (T_{g1} - T_g(\xi) + C_2) + D(T_g(\xi) - C_2)]} \tag{18}$$

If we consider $T_g(\xi)$=T_{g1} in the case of fully cured material ($\xi = 1$) it follows from Eq. (18):

$$x_0 - 1 = \frac{C_2}{C_2 \log(\tau_0/\tau_{s0}) + D(T_{g1} - C_2)} \tag{19}$$

Using this equation we can substitute $\log(\tau_0/\tau_{s0})$ in Eq. (18):

$$\xi = x_0 - \frac{T_{g1} - T_g(\xi) + C_2}{[(1/(x_0 - 1) - D(T_{g1} - C_2)/C_2) \times (T_{g1} - T_g(\xi) + C_2) + D(T_g(\xi) - C_2)]} \tag{20}$$

If we consider $T_g(\xi) = T_{g0}$ (i.e. the glass transition temperature of the initial mixture) for $\xi = 0$ follows from Eq. (20):

$$0 = x_0 - \frac{T_{g1} - T_{g0} + C_2}{[(1/(x_0 - 1) - D(T_{g1} - C_2)/C_2) \times (T_{g1} - T_{g0} + C_2) + D(T_{g0} - C_2)]} \quad (21)$$

This equation yields a quadratic equation in x_0 with the solution:

$$x_0 = \frac{1}{2} + \sqrt{\frac{1}{4} + \frac{C_2(T_{g1} - T_{g0} + C_2)}{DT_{g1}(T_{g1} - T_{g0})}} \quad (22)$$

By transformation of Eq. (20) the dependence of T_g from ξ is

$$T_g(\xi) = T_{g1} + C_2 - \frac{DT_{g1}}{1/(x_0 - 1) - (DT_{g1}/C_2) - 1/(x_0 - \xi)} \quad (23)$$

The combination of Eqs. (22) and (23) is the resulting expression for the conversion dependence of the glass transition temperature. To describe this behavior four parameters are needed. T_{g0} and T_{g1} can be easily determined by separate DSC experiments. The fit parameters D and C_2 are also parameters of the activation curve of the thermal relaxation of the uncured material.

The derived function $T_g(\xi)$ given by Eqs. (22) and (23) is verified by the data set (T_τ, ξ) determined from the measurements is shown in Fig. 5. These values determined by a frequency dependent experiment (T_τ) are of course not identical to the glass transition temperature T_g measured by DSC at 10 K/min. However, the determination of T_g for partially cured material is relatively uncertain because of the enthalpy relaxation peak and the post-curing reaction, which already begins in the glass transition range (see Fig. 3). The values of T_τ can be determined more accurately. In the case of quasi-isothermal TMDSC experiments, it is identical to the curing temperature. As shown in Fig. 12, the difference between T_τ (filled circles) and T_g (open circles) is small under the experimental conditions used. The data of T_τ and T_g are taken from the measurements is shown in Figs. 5 and 3, respectively. For the discussion of the validity of Eq. (23) only the T_τ data are used. In Eqs. (22) and (23) we therefore have to replace T_{g0} with $T_{\tau 0}$, T_{g1} with $T_{\tau 1}$ and $T_g(\xi)$ with $T_\tau(\xi)$.

For the partially cured material the values of T_τ are taken from the quasi-isothermal TMDSC measurements. The values for the uncured and the fully cured material are determined by separate TMDSC experiments with an underlying heating rate of 0.5 K/min and a frequency of 42 mHz. The results are $T_{g0} = -14.4\ ^\circ$C (for the uncured material) and $T_{g1} = 170.6\ ^\circ$C (for the fully cured material). Using the combination of Eqs. (22) and (23) the data have been fitted under different conditions. The fit results are listed in Table 1. The use of these parameters Eq. (22) gives values of x_0 between 1.058 and 1.029. These values are a little lower than the fit result presented in Fig. 11 ($x_0 = 1.069$). The best agreement between the measured data and the fit curves yield values of T_{g1} larger than the measured value of the fully cured material (170.6 °C). This is an indication of the experimental uncertainty of this parameter. As reported by Montserrat [45], the glass transition temperature of the fully cured material depends on the curing conditions. The parameters D and C_2 from Table 1 show very good agreement with the values determined by the fit of the relaxation curve of the uncured material ($D = 2.178$ and $C_2 = 29.35$ K). This agreement is an indication of the applicability of the present concept to describe the relation between the glass transition temperature and the conversion on the basis of the relaxation behavior.

As described above, the values of T_τ instead of T_g are used for the verification of Eq. (23). Here we discuss the influence of the differences between T_τ and T_g on the parameters of Eq. (23) in more detail. The values of T_g for the uncured and the fully cured material are determined by independent DSC measurements at 10 K/min. For the determination of T_g the fictive temperature method (Richardson method [46]) is used and the average of cooling and heating runs are taken. The results are $T_{g0} = -18.3\ ^\circ$C and $T_{g1} = 166.5\ ^\circ$C. The comparison with the related values of T_τ ($T_{\tau 0} = -14.4\ ^\circ$C and $T_{\tau 1} = 170.6\ ^\circ$C) shows that the glass transition temperature for both kinds of material is 4 K lower than the temperature of the relaxation transition (T_τ) at 42 mHz. As a result of this, the values of D and C_2 do not vary for the case that T_τ is used instead of T_g in Eq. (23).

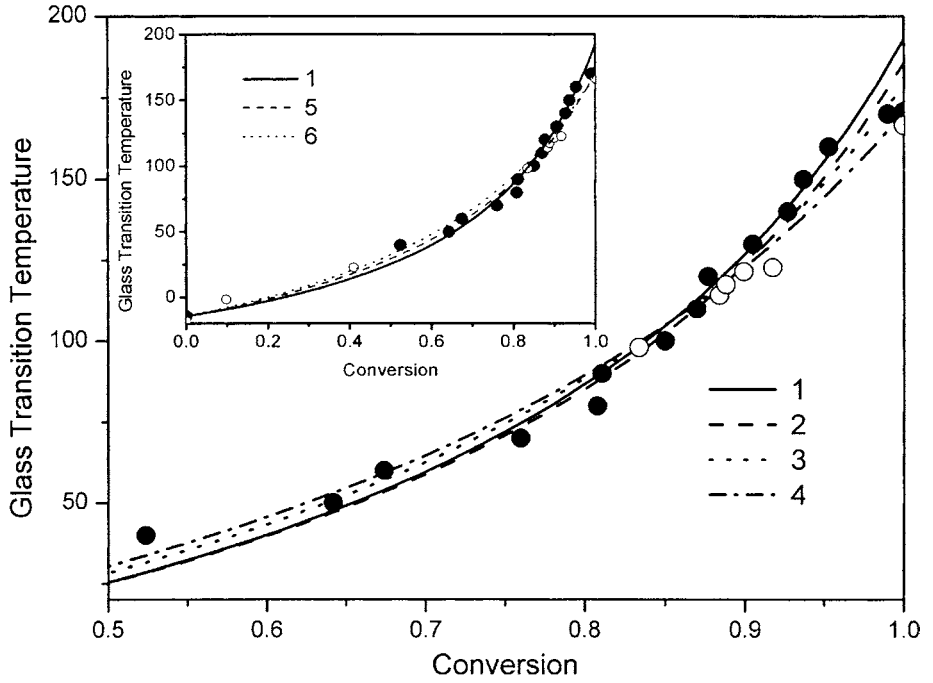

Fig. 12. The glass transition temperature as a function of conversion. The filled circles are taken from TMDSC experiments. For comparison, the values from conventionally DSC (from Fig. 4) are also plotted (open circles). The curves represent different fit-curves. The different curves are described in Table 1. In the inset the data are plotted over the whole conversion range.

Finally, the quality of the description of the function $T_g(\xi)$ (or $T_\tau(\xi)$) on the basis of Eqs. (22) and (23) is compared with relationships taken from the literature. For this comparison we selected the frequently used DiBenedetto equation [15,47]:

$$T_g(\xi(t_{react})) = \frac{\lambda\xi(t_{react})(T_{g1} - T_{g0})}{1 - (1-\lambda)\xi(t_{react})} + T_{g0} \qquad (24)$$

where λ is a fit parameter. By curve fitting of the data in Fig. 12 we get $\lambda = 0.31$. The resulting curve is practically identical to the fit curve from Eq. (23).

The fit parameter λ can be linked to the relation of the heat capacity change at the glass transition $\lambda = \Delta c_{p1}/\Delta c_{p0}$ [47], where Δc_{p1} and Δc_{p0} are the c_p change of the fully cured and uncured material, respectively. We measured these differences to be $\Delta c_{p1} = 0.20$ J/g K and $\Delta c_{p0} = 0.59$ J/g K by conventional DSC, giving $\lambda = 0.34$. The curve calculated with this parameter deviates from the best fit curves. However, this curve also fits the experimental data reasonably well. The related fit curves are the curves 5 and 6 is shown in Fig. 12.

Table 1
Fit parameters of the curves are shown in Fig. 12

Curve	T_{g0} (°C)	T_{g1} (°C)	C_2 (K)	D	Remarks
	−14.4		29.35	2.178	VF fit of the data in Fig. 2
1	−14.4	193.0	27.5	2.272	Fit using Eq. (23) without the data at $\xi \approx 1$ (best fit of the measured data)
2	−14.4	189.7	29.35	2.178	Fit using Eq. (23) with the VF parameter (the only fit parameter is T_{g1})
3	−14.4	179.0	33.0	1.900	Fit of all the data using Eq. (23)
4	−14.4	170.6	38.1	1.693	Fit using Eq. (23) with the measured value of T_{g1}
5	−14.4	170.6			DiBenedetto equation with $\lambda = 0.31$
6	−14.4	170.6			DiBenedetto equation with $\lambda = 0.34$

In Fig. 12 the fitting results of Eqs. (23) and (24) show small differences. However, Eq. (23) is consistent with the concept of the relaxation behavior in chemically unstable material. This concept describes the shape of the heat capacity curve during reactions, the change of the thermal relaxation time during reactions, the vitrification process [17,18] and now the conversion dependence of the glass transition temperature. For all these effects the same set of parameters (D, C_2, T_{g0}, T_{g1}) can be used. The parameter can be determined by different independent experiments.

5. Conclusions

In the concept of the thermal relaxation of chemically unstable materials, the change of the relaxation time during the curing reaction of the DGEBA–DDM system can be described in the same way as a cooling experiment of chemically stable material. In this approach, the fictive cooling rate is given by the rate of reaction. Applying this approach to the conversion dependence of the glass transition temperature yields a new equation. The parameters in this equation are related to the relaxation behavior of the uncured material. The fragility parameter D and the Vogel temperature T_v of the VF equation for thermal relaxation can thus be estimated from the T_g–ξ diagram. Furthermore, it is shown that the TMDSC measurements of the heat capacity during reactions yield additional information on the reaction kinetics and the mechanism of cross-linking.

The results presented in this work assume relaxation processes in a more or less equilibrated liquid. For simplification, we have not extended this work non-equilibrium conditions (vitrification). However, the procedure can easily be extended to non-equilibrium conditions. Such an extension makes the relationships more complex and would probably yield only insignificant improvements in the examples discussed.

Acknowledgements

The author would like to thank Ingo Alig (Deutsches Kunststoff Institut, Darmstadt) for providing the dielectric data and is grateful to Rudolf Riesen (Mettler-Toledo GmbH, Schwerzenbach) and Silvia Corezzi (University of Perugia) for helpful discussions.

References

[1] W.F. Hemminger, G.W.H. Höhne, Calorimetry, Verlag Chemie, Weinheim, 1984.
[2] G.W.H. Höhne, J. Therm. Anal. 37 (1991) 1987.
[3] G.W.H. Höhne, J.E.K. Schawe, C. Schick, Thermochim. Acta 221 (1993) 129.
[4] G.W.H. Höhne, H.K. Cammenga, W. Eysel, E. Gmelin, W. Hemminger, Thermochim. Acta 160 (1990) 1;
H.K. Cammenga, W. Eysel, E. Gmelin, W. Hemminger, G.W.H. Höhne, S.M. Sarge, Thermochim. Acta 219 (1993) 333;
S.M. Sarge, E. Gmelin, G.W.H. Höhne, H.K. Cammenga, W. Hemminger, W. Eysel, Thermochim. Acta 247 (1994) 129.
[5] G.W.H. Höhne, Thermochim. Acta 187 (1991) 283.
[6] J.E.K. Schawe, C. Schick, G.W.H. Höhne, Thermochim. Acta 244 (1994) 49.
[7] M.J. Richardson, Pure Appl. Chem. 64 (1992) 1789.
[8] G.W.H. Höhne, W. Hemminger, H.J. Flammersheim, Differential Scanning Calorimetry, Springer, Berlin, 1996.
[9] H. Gobrecht, K. Hamann, G. Willers, J. Phys. E 4 (1971) 21.
[10] M. Reading, D. Elliott, V.L. Hill, J. Therm. Anal. 40 (1993) 949.
[11] M. Cassettari, G. Salvetti, E. Tombari, S. Veronesi, G.P. Johari, Il Nuovo Cimento D 14 (1992) 763.
[12] J.E.K. Schawe, Thermochim. Acta 261 (1995) 183.
[13] G. Van Assche, A. Van Himelrijck, H. Rahier, B. Van Mele, Thermochim. Acta 268 (1995) 121.
[14] G. Van Assche, A. Van Himelrijck, H. Rahier, B. Van Mele, Thermochim. Acta 286 (1996) 209.
[15] A.T. DiBenedetto, J. Polym. Sci. 25 (1987) 1949.
[16] C. Ferrari, G. Salvetti, E. Tombari, G.P. Johari, Phys. Rev. E 54 (1996) R1058.
[17] J.E.K. Schawe, I. Alig, Coll. Polym. Sci. 279 (2001) 1169.
[18] J.E.K. Schawe, I. Alig, J. Chem. Phys., submitted for publication.
[19] B. Wunderlich, Y. Jin, A. Boller, Thermochim. Acta 238 (1994) 277.
[20] J.E.K. Schawe, Thermochim. Acta 304/305 (1997) 111.
[21] S. Weyer, A. Hensel, C. Schick, Thermochim. Acta 304/305 (1997) 267.
[22] J.E.K. Schawe, Thermochim. Acta 361 (2000) 97.
[23] H. Vogel, Physik. Z. 22 (1921) 645.
[24] G.S. Fulcher, J. Am. Chem. Soc. 8 (1923) 339.
[25] C.A. Angell, J. Non-Cryst. Solids 131–133 (1991) 13.
[26] C.T. Moynihan, P.B. Macedo, C.T. Montrose, P.K. Gupta, M.A. DeBolt, J.F. Dill, B.E. Dom, P.W. Drake, A.J. Easteal, P.B. Elterman, R.P. Moeller, H. Sasabe, J.A. Wilder, Ann. NY Acad. Sci. 279 (1976) 15.
[27] K. Schneider, E. Donth, Acta Polym. 37 (1986) 333.
[28] A. Hensel, J. Dobbertin, J.E.K. Schawe, A. Boller, C. Schick, J. Therm. Anal. 46 (1996) 935.

[29] H. Huth, M. Beiner, S. Weyer, M. Merzlyakov, C. Schick, E. Donth, Thermochim. Acta 377 (2001) 113.
[30] G. Wisanrakkit, J.K. Gillham, J. Appl. Polym. Sci. 41 (1990) 2885.
[31] J.E.K. Schawe, J. Thermal. Anal. Cal. 64 (2001) 599.
[32] A. Van Hemelrijck, B. Van Mele, J. Therm. Anal. 49 (1997) 437.
[33] S. Montserrat, I. Cima, Thermochim. Acta 330 (1999) 189.
[34] J.K. Gillham, Polym. Eng. Sci. 26 (1986) 1429.
[35] B. Wunderlich, Thermal Analysis, Academic Press, Boston, 1990, p. 240 ff.
[36] R. Pan, M. Varma-Nair, B. Wunderlich, J. Therm. Anal. 35 (1989) 955.
[37] V.A. Bershtein, V.M. Egorov, L.M. Egorova, V.A. Ryshov, Thermochim. Acta 238 (1994) 41.
[38] B.D. Fitz, I. Mijovic, Macromolecules 32 (1999) 4134.
[39] B.D. Fitz, I. Mijovic, Macromolecules 32 (1999) 3518.
[40] G.P. Johary, J. Macromol. Liq. 56 (1993) 153.
[41] E. Tombari, G.P. Johary, J. Chem. Phys. 97 (1992) 6677.
[42] G. Adam, J.H. Gibbs, J. Chem. Phys. 43 (1965) 139.
[43] S. Corezzi, personal information.
[44] S.L. Simon, J.K. Gillham, J. Appl. Polym. Sci. 47 (1993) 461.
[45] S. Montserrat, personal information.
[46] M. Richardson, in: G. Allen (Ed.), Comprehensive Polymer Science, Vol. 1, Pergamon Press, Oxford, 1989, p. 867 ff.
[47] J.P. Pascault, R.J.J. Williams, J. Polym. Sci. Polym. Phys. Ed. 28 (1990) 85.